MEG Multipolar Modeling of Distributed Sources Using RAP-MUSIC

John C. Mosher[1], Sylvain Baillet[2], Karim Jerbi[3,4], Richard M. Leahy[3],
[1]Los Alamos National Laboratory, Los Alamos, NM USA
[2]Cognitive Neuroscience & Brain Imaging Laboratory, Hôpital de la Salpêtière, CNRS, Paris, France;
[3]Signal & Image Processing Institute, University of Southern California, Los Angeles, CA USA
[4]Biomedical Engineering Institute, University of Karlsruhe, Germany

Abstract

We describe the use of truncated multipolar expansions for producing dynamic images of cortical neural activation from measurements of the magnetoencephalogram. We use a signal-subspace method to find the locations of a set of multipolar sources, each of which represents a region of activity in the cerebral cortex. Our method builds up an estimate of the sources in a recursive manner, i.e. we first search for point current dipoles, then magnetic dipoles, and finally first order multipoles. The dynamic behavior of these sources is then computed using a linear fit to the spatio-temporal data. The final step in the procedure is to map each of the multipolar sources into an equivalent distributed source on the cortical surface. The method is illustrated through an application to epileptic interictal MEG data.

1. Introduction

Magnetoencephalography (MEG) data are measurements of the magnetic fields produced by neural current sources within the brain. The problem of estimating these sources is highly ill-posed due to the inherent ambiguities in the associated quasistatic electromagnetic inverse problem, the limited number of spatial measurements and significant noise levels. To overcome these problems, constraints can be placed on the location and form of the current sources. Mapping studies using direct electrical measurements, fMRI and PET reveal discrete focal areas of strong activation within the cortex that are associated with specific cognitive, sensory and motor activities. Consequently, a plausible model for the current generators in an event related study consists of a number of focal cortical regions each of which has an associated time course. The MEG inverse problem requires estimation of the spatial and temporal characteristics of these sources.

This work was supported in part by the National Institute of Mental Health Grant R01-MH53213, and by Los Alamos National Laboratory, operated by the University of California for the United States Department of Energy under contract W-7405-ENG-36.

The model-based methods assume a specific parametric form for the sources. By far the most widely used models in MEG are multiple current dipoles [1], [7]. These assume that the neural sources are relatively small in number and each sufficiently focal that they can be represented by a few equivalent current dipoles with unknown locations and orientations. Parametric methods can be extended to model the temporal correlation expected in the solutions through fitting the multiple dipole model to the entire data set and estimating the time course for each estimated dipole location. As with most nonlinear imaging methods, the cost functions are nonconvex. Signal subspace based methods such as MUSIC or RAP-MUSIC [7] can be used to rapidly locate the sources in a sequential fashion and avoid the problem of trapping in local minima.

An alternative approach reviewed in [5], [6] is to extend the parametric source representations within the model-based framework to allow for distributed sources. The multipolar expansion of the magnetic field about the centroid of a distributed source readily offers an elegant parametric model, which collapses to a dipole model in the limiting case and includes higher order terms in the case of a spatially extended source. While multipolar expansions have been applied to magnetocardiography (MCG) source modeling [4], their use in MEG has been restricted to simplified models [9]. The physiological interpretation of these higher-order components in non-intuitive, therefore limiting their application in this community (cf. [11]).

The method described here for estimating the location and moment parameters of these multipolar representations is an extension of the RAP-MUSIC method developed in [7] for localizing current dipoles. The algorithm recursively builds a model for the current source configuration by first testing for the presence of point current dipoles, then magnetic dipoles, and finally first order multipoles. In this way the model order and complexity is gradually increased until the combined estimated sources adequately explain the data.

0-7803-6514-3/00/$10.00©2000 IEEE

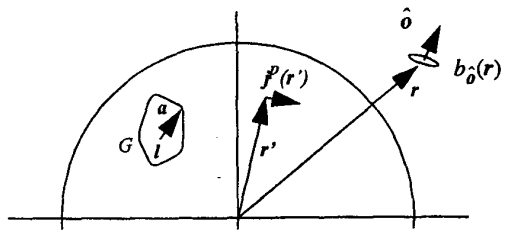

Fig. 1: Primary neural activity of current density $j^p(r')$ at location r' inside a closed conducting volume generates a total current field within the volume that in turn generates an external magnetic field at location r, as detected by a magnetometer with sensor orientation $\hat{o}$, to yield the scalar magnetic measurement $b_{\hat{o}}(r)$. At location l we consider a small region G of primary neural activity, whose volume is spanned by a. Thus $r' = l + a$ within this region.

In the cortical re-mapping stage, we find regions of cortex in the vicinity of the parametric source on which we fit current distributions consistent with the fields associated with each estimated multipole. The final result is then a dynamic image of current activity mapped onto a tessellated representation of the cortex which reveals the time varying behavior at the various locations on the cerebral cortex activated during a particular experiment.

In this study we extend the results of [5] by presenting the case of arbitrarily oriented sensors outside a conducting sphere, then present the application of this model to experimental data.

2. Methods

2.1. MEG Multipolar Expansions for Radial Case

The external magnetic field is generated by the sum of the *primary neural activity*, designated by the current density vector $j^p(r')$, and the *volume* or *return currents* resulting from the electric field produced by the current source. It is the primary currents that are the sources of interest in MEG inverse problems [1]. In the special case of radial measurements for sources confined to a spherical volume, the volume currents do not contribute to the measured field, and the radial component $b_r(r)$ of the magnetic field $b(r)$ at location r is given by the well known equation:

$$b_r(r) \equiv \frac{r \cdot b(r)}{r} = \frac{r}{r} \cdot \frac{\mu_0}{4\pi} \int_V M(r') / d^3(r, r') dr' \qquad (1)$$

where $d(r, r') = r - r'$ is the distance vector between the sensor and source locations, $d(r, r') = \|r - r'\|$ the corresponding scalar distance, r/r is a unit vector pointing in the radial direction, and V is any volume containing the primary source activity. We define the *magnetic moment density* or *magnetization* as $M(r') \equiv r' \times j^p(r')$, [2], [8].

In the geometry of Fig. 1, the external magnetic field is generated by an arbitrary *primary neural activity* designated by the current density vector $j^p(r')$ (nA/m^2), independent of the origin. We restrict the primary current to a small volume G, centered about point l, as shown in Fig. 1. In the sequel, we will find the following expansions and gradients useful. Let ∇ indicate the gradient with respect to the unprimed variable r. The first order multipolar representation is derived using a truncated Taylor series expansion of the distance $d(r, r')$ about $r' = r_l$, the centroid of the region to which the primary source is confined. A scalar function can be approximated using the Taylor Series Expansion as

$$\psi(r' + a) = \sum_{n=0}^{\infty} \frac{1}{n!} (a \cdot \nabla')^n \psi(r') \qquad (2)$$

and expanding for the first two terms yields

$$\psi(r' + a) = \psi(r') + a \cdot \nabla' \psi(r') + \ldots \qquad (3)$$

where the notation ∇' indicates the gradient with respect to the primed variable r'. Using the equalities $\nabla r = I$ where I is the identity matrix, $\nabla r^n = \nabla (r \cdot r)^{n/2} = n r^{n-2} r$ and $\nabla d^n = -\nabla' d^n = n d^{n-2} d$, yields the expansions:

$$d(r, r' + a)^{-1} = d(r, r')^{-1} + d(r, r')^{-3} (a \cdot d(r, r')) + \ldots \quad (4)$$

$$d(r, r' + a)^{-3} = d(r, r')^{-3} + 3 d(r, r')^{-5} (a \cdot d(r, r')) + \ldots \quad (5)$$

Thus if $a \ll d(r, r')$ we may neglect the second and higher terms. From Fig. 1 we observe that this inequality is equivalent to the extent of the distributed source being much smaller than the distance from the source to the sensor point. A practical application is to cortical sources that have a spatial extent that is relatively small compared to the distance to the sensor array, as illustrated in Fig. 2.

We truncate the series after the 1st-order term, with the assumption that $x^2 \ll d(r, r_l)^3$, which is to say that the source does not have a large radius relative to the distance to the observation point. Inserting *(5)* into *(1)* yields the magnetic multipolar expansion

$$b_r(r) \equiv \frac{\mu_0}{4\pi} \frac{r}{r \|r - r_l\|^3} \cdot \left(\int M(r_l + x) dx + \frac{3}{\|r - r_l\|^2} \left(\int M(r_l + x) x dx \cdot (r - r_l) \right) \right) \qquad (6)$$

where the integration is carried out over the volume of the primary source activity, centered on r_l.

2.1.1. Equivalent Magnetic Moment (EMM): Let the extent of the primary source activity V be sufficiently small that the second term in the multipolar expansion is negligible. As shown in [5], we can rewrite *(6)* as

$$b_r(r) = \frac{r}{r} \cdot \frac{\mu_0}{4\pi} \int \frac{M(r_l + x)}{\|r - r_l\|^3} dx = \frac{\mu_0}{4\pi} \frac{r \cdot m}{r\|r - r_l\|^3} \quad (7)$$

where we define m to be the *magnetic moment*

$$m(r_l) \equiv \int (r_l + x) \times j^p(r_l + x) dx . \quad (8)$$

Furthermore, if we define $q(r_l) \equiv \int j^p(r_l + x) dx$ to be the *equivalent current dipole*, we can express *(8)* as

$$m(r_l) = r_l \times q(r_l) + \tilde{m}(r_l) \quad (9)$$

where $\tilde{m}(r_l) \equiv \int x \times j^p(r_l + x) dx$ is the magnetic dipole moment centered at r_l due to the primary current density. Thus this model includes the equivalent current dipole as a limiting case where the source either has virtually no spatial extent or no net magnetic dipole moment.

2.1.2. First-Order Multipole: If the spatial extent of the source is sufficiently large, then we retain the first two terms in the Taylor series and rewrite *(6)* as

$$b_r(r) \equiv \frac{\mu_0}{4\pi} \cdot \frac{r}{rd^3(r, r_l)} \cdot \left(m(r_l) + \frac{3(Q(r_l) \cdot d(r, r_l))}{d^2(r, r_l)} \right) \quad (10)$$

where $Q(r_l)$ is the magnetic quadrupolar term defined as the 3×3 tensor product $Q(r_l) \equiv \int M(r_l + x) x dx$. We can rewrite this tensor using the Kronecker product $a \otimes b$, defined as the concatenation of the product of each element of a with the vector b, and the operator vec(A), defined as the concatenation of the columns of a matrix A into a vector:

$$b_r(r) \equiv \frac{\mu_0}{4\pi} \left(\frac{r}{rd^3(r, r_l)} \cdot m + \frac{3(d(r, r_l) \otimes r)}{rd^5(r, r_l)} \cdot \text{vec}(Q) \right) \quad (11)$$

where for notational convenience we drop the dependency of m and Q on r_l. We therefore characterize the first-order multipole using the combination of the three magnetic moment vector m, the nine magnetic quadrupolar terms in Q, and the location r_l.

2.2. Expansions for Arbitrary Orientations

We define another useful function [10]

$$F(r, r') \equiv rd^2 + (r \cdot d)d , \quad (12)$$

then

$$F^{-1}(r, r' + a) = F^{-1}(r, r') - (a \cdot \nabla' F(r, r')) F^{-2}(r, r') + \ldots \quad (13)$$

where

$$-\nabla' F = \left(2r + \frac{(r \cdot d)}{d} \right) d + rd . \quad (14)$$

Other useful gradients are the vector

$$\nabla F(r, r') = \left(\frac{d^2}{r} + d \right) r + \left(2r + \frac{(r \cdot d)}{d} + d \right) d \quad (15)$$

and the matrix

$$-\nabla(\nabla' F(r, r')) = \left(2r + \frac{(r \cdot d)}{d} + d \right) I + \frac{rd}{d} + d \left(\frac{2r}{r} + \frac{(d + r)}{d} - \frac{(r \cdot d)d}{d^3} \right) \cdot \quad (16)$$

The magnetic field outside a sphere due to a magnetization density $M(r')$ is given by [10]

$$b(r) = \frac{-\mu_0}{4\pi} \int_G \nabla \left(\frac{M(r') \cdot r}{F(r, r')} \right) dr' , \quad (17)$$

where the function F is defined in (12). Substituting just the first term of the expansion (13) yields

$$b(r) \equiv \frac{-\mu_0}{4\pi} \int_G \nabla \left(\frac{M(l + a) \cdot r}{F(r, l)} \right) da = \frac{-\mu_0}{4\pi} \nabla \left(\frac{r \cdot m}{F(r, l)} \right) . \quad (18)$$

Expanding the gradient and applying the sensor orientation $\hat{o}$ yields the focal dipole model

$$b_{\hat{o}}(r) = \frac{\mu_0}{4\pi} \left(\frac{(\nabla F(r, l) \cdot \hat{o}) r}{F^2(r, l)} - \frac{\hat{o}}{F(r, l)} \right) \cdot m . \quad (19)$$

where $\nabla F(r, l)$ is defined in (15).

As before, we can equivalently express the solution as the sum of a current dipole and a local magnetic dipole $m(l)$, where the point current dipole model is expressed as the well-known solution [10],

$$b_{\hat{o}}(r) = \frac{\mu_0}{4\pi} \left(\frac{(\nabla F(r, l) \cdot \hat{o})(r \times l)}{F^2(r, l)} - \frac{\hat{o} \times l}{F(r, l)} \right) \cdot q . \quad (20)$$

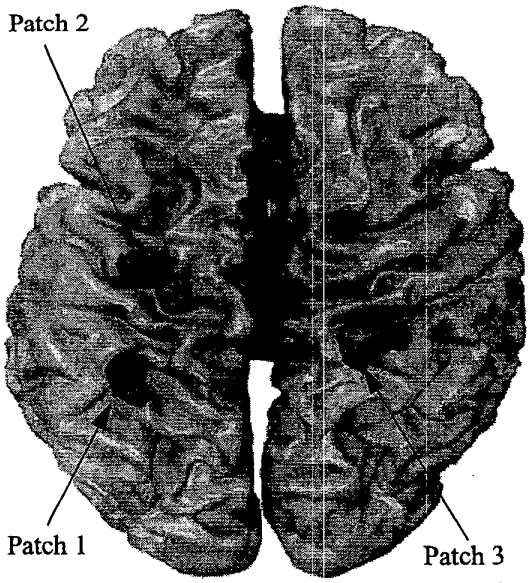

Fig. 2: A tessellated human cortex showing mappings of three sources onto the cortical surface. The radius of the patches is small relative to the distance to the sensor array.

2.3. First-order Multipole

Retaining the first two terms of $F^{-1}(r, r')$ yields the first-order approximation

$$b(r) \equiv \frac{-\mu_0}{4\pi} \nabla \left(\frac{r \cdot m}{F(r, l)} - \frac{r \cdot Q_m \cdot \nabla' F(r, l)}{F^2(r, l)} \right) \tag{21}$$

The gradient of the second term yields (suppressing the dependence of F on its parameters)

$$\nabla \left(\frac{r \cdot Q_m \cdot \nabla' F}{F^2} \right) =$$

$$\frac{F^2 (r \cdot Q_m \cdot \nabla \nabla' F + Q_m \cdot \nabla' F)}{F^4} - \tag{22}$$

$$\frac{(r \cdot Q_m \cdot \nabla' F(r, l)) 2F \nabla F}{F^4}$$

and constraining to the sensor orientation $\hat{o}$ yields

$$= F^{-2} (r \cdot Q_m \cdot (\nabla \nabla' F \cdot \hat{o}) + \hat{o} \cdot Q_m \cdot \nabla' F) - \tag{23}$$

$$2F^{-3} (r \cdot Q_m \cdot \nabla' F)(\nabla F \cdot \hat{o})$$

Finally collecting similar terms yields

$$b_{\hat{o}}(r) \equiv b(r) \cdot \hat{o} \equiv \frac{\mu_0}{4\pi} \left(\left(\frac{(\nabla F \cdot \hat{o}) r}{F^2} - \frac{\hat{o}}{F} \right) \cdot m \right) +$$

$$\frac{\mu_0}{4\pi} (F^{-2} [(\nabla \nabla' F \cdot \hat{o}) \otimes r + \nabla' F \otimes (\hat{o} - 2F^{-1} (\nabla F \cdot \hat{o}) r)] \cdot \tag{24}$$

$$\text{vec}(Q_m))$$

where $\nabla' F$, ∇F, and $\nabla \nabla' F$ are given by (14), (15), and (16) respectively.

3. Experimental Application

In our previous work [5], [6], [7], we have showed the applicability of these multipolar expansions using RAP-MUSIC to combinations of simulated and phantom data. In [3], we showed through Cramer-Rao error analysis and Monte Carlos studies the applicability of the magnetic moment in localizing current dipole activity, i.e., the magnetic moment model did not reveal increased error when applied to a current dipole source. We present here the application of the current and magnetic dipolar expansions to an experimental data comprising epileptic interictal activity.

We collected spontaneous MEG data over five minutes on a 68-channel 1st-order axial gradiometer system. The data channels were then manually scanned for spike activity in the temporal waveshapes, and identified regions were extracted for localization analysis. A rank of 13 visibly indicated a good partition between signal and noise subspaces over the selected 180 milliseconds, but other ranks were

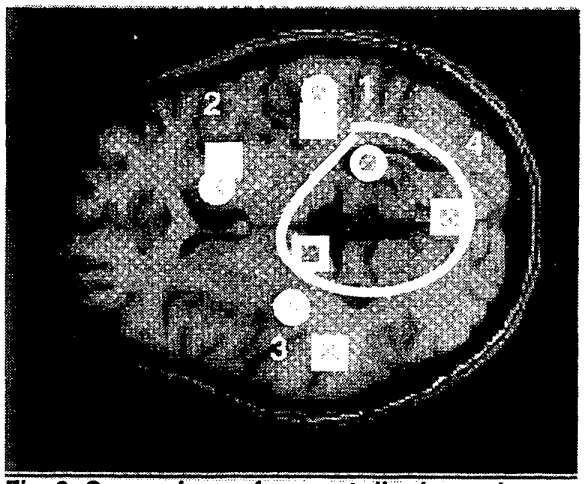

Fig. 3: Comparison of current dipolar and magnetic moment models, applied to interictal activity. Sources have been overlaid into a transaxial slice centered in the brain. The four circles indicate the current dipole solution, and the five squares indicate the magnetic moment solution, applied to the same data. The principle difference in the two solutions lies in the circled region, numbered "4." Most of the solutions (varied over rank, correlation, and time period) indicate 4 and 1 initiate the interictal activity, with near simultaneous transfer to 3, followed by 2. Depth electrodes have been inserted in the vicinity of 1 and 4 to confirm activity, but further research and simulation are required to understand the differences in these models.

investigated as well. The RAP-MUSIC correlation cutoff was selected as 0.95, and a strong Tikhonov regularizer was applied to the solutions.

Analysis of the MEG data revealed epileptiform activity posterior to the somatosensory cortex, as discussed in Fig. 3. Critical to the evaluation of epilepsy is the sequence of events. Application of the current and dipolar models yields similarities yet important differences in the interpretation of the results. Both models indicate a propagation from the posterior to anterior regions, and both appear to indicate a propagation from right to left. The initiation site, however, is unclear due to the source complexity in the time instances leading up to the spikes.

Because these source models are only approximate and the underlying physics ambiguous, then determination of which solution is "better" will require close collaboration with neurologists. The challenge is to rigorously incorporate their subjective information into the solution, without overprescribing the answer.

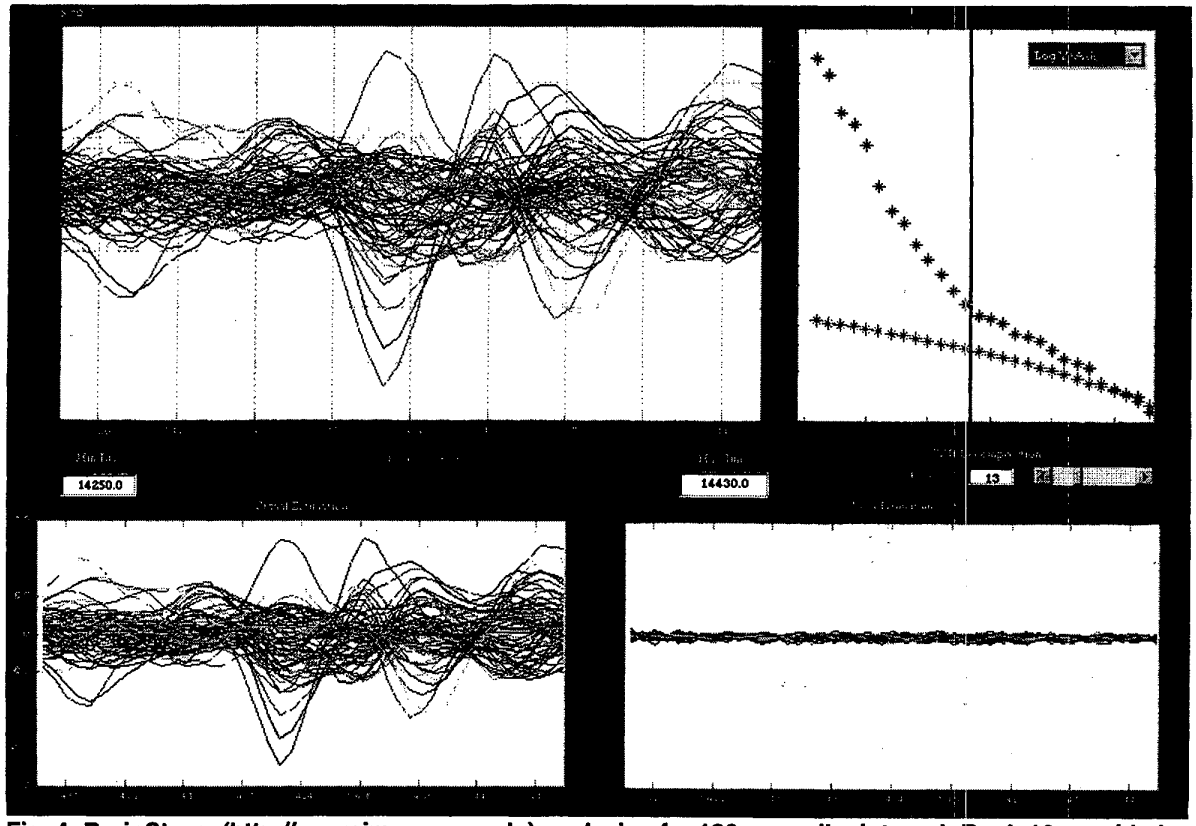

Fig. 4: BrainStorm (http://neuroimage.usc.edu) analysis of a 180 ms spike interval. Rank 13 provided a conservative separation between signal (bottom left) and noise (bottom right) subspaces. Other ranks yielded similar localization results in the current dipole and magnetic moment models. Detailed observations of the sensor waveshapes reveals several simultaneous independent events occurring.

References

[1] Hämäläinen M, Hari R, Ilmoniemi RJ, Knuutila J, Lounasmaa OV, "Magnetoencephalography-Theory, Instrumentation, and Applications of Noninvasive Studies of the Working Human Brain" *Rev. Mod. Phys.* vol. 65, pp. 413–497, March, 1993. New York, 1989, pp. 3–18.

[2] Jackson JD, *Classical Electrodynamics, Second Edition,* John Wiley & Sons:New York, 1975.

[3] Jerbi K, Mosher JC, Baillet S, Leahy RM, "Error Bounds in MEG Multipole Localization," *Proceedings of the Twelfth Conference on Biomagnetism*, Helsinki, Finland, August 2000, in press.

[4] Katila TE and Karp PJ, "Magnetocardiography: Morphology and Multipole Presentations", in *Biomagnetism: An Interdisciplinary Approach*, S.J. Williamson, G.L. Romani, L. Kaufman and I. Modena, Eds. New York: Plenum, 1983.

[5] Mosher JC, Leahy RM, Schattuck DW and Baillet S, "MEG Source Imaging Using Multipolar Expansions", *Proc. IPMI99*, Springer Verlag, *Lecture Notes in Computer Science*, 1999, pp. 98-111.

[6] Mosher JC, Baillet S, Leahy RM, "EEG source localization and imaging using multiple signal classification approaches," *J. Clinical Neurophysiology*, invited paper, Vol. 16, pp 225-238, 1999.

[7] Mosher JC, Leahy RM, "Source Localization Using Recursively Applied and Projected (RAP) MUSIC", *IEEE Trans. Signal Proc.*, Vol 47, 1999, pp. 332-340.

[8] Nenonen J, Katila T, Leinio M, Montonen J, Makijarvi M, Siltanen P, "Magnetocardiographic functional localization using current multipole models," *IEEE Trans. Biomed. Eng.*, vol 38, no. 7, July 1991, pp. 648–657.

[9] Nolte Gand Curio G, "On the Calculation of Magnetic Fields based on Multipole Modeling of Focal Biological Sources", in *Biophysical Journal*, Vol. 73, 1997, pp. 1253-1262.

[10] Sarvas J., 1987, "Basic mathematical and electromagnetic concepts of the biomagnetic inverse problem," *Phys in Med Biol*, vol. 32, pp. 11-22.

[11] Wikswo JP, Swinney KR, "Scalar multipole expansions and their dipole equivalents," *J. Appl. Phys.* vol. 57 (9), 1 May 1985, pp. 4301–4308.